ENCIT 2018

ABCM Associação Brasileira de Engenharia e Ciências Mecânicas

17th Brazilian Congress of Thermal Sciences and Engineering
November 25th-28th, 2018, Águas de Lindóia, SP, Brazil

ENCIT-2018-XXXX
BOUNDARY LAYER TRANSITION FROM SMOOTH TO ROUGH WALLS

Gabriel Maltese Meletti
Brandenburg University of Technology Cottbus Senftenberg – BTU
Siemens-Halske-Ring 14, 03046, Cottbus, Germany
gabriel.meletti@b-tu.de

Erick de Moraes Franklin
School of Mechanical Engineering – University of Campinas – UNICAMP
Rua Mendeleyev 200, 13083-860, Campinas, SP, Brazil
franklin@fem.unicamp.br

Abstract. *This paper presents an experimental study on the channel flow transition from smooth to rough walls, and also the transition back to the smooth region. Different water flow rates were imposed in a closed conduit of rectangular cross section, where rough elements consisting of cavities of d- and k-type covered part of the bottom wall of the test section. These transitions cause a shift on flow velocity profiles that changes their parameters when compared to the flow over a smooth wall. Reynolds numbers based on the channel half-height were moderate, varying between 7800 and 9600, and the regime upstream of the rough elements was hydraulically smooth. Experimental data for this specific case remain scarce and the physics involved rests to be better understood. The flow field was measured using low frequency PIV (particle image velocimetry). From the instantaneous fields measured with PIV, the mean velocities, fluctuations, shear stresses and turbulence production were computed. The results show the presence of oscillations in Reynolds stress and turbulence production, that are higher for the k-type roughness, and were not shown in previous experimental works.*

Keywords: *Boundary layer, Turbulence, Roughness, Transition*

1. INTRODUCTION

Turbulent boundary layers over rough elements are frequently found in nature and industry. One example in nature is the air flow over cities, when wind blows over buildings and houses that can be considered as rough elements. In industry, a common example is the turbulent flow in pipes and closed conduits with rough walls, such as happens, for instance, in chemical and oil industries. The presence of rough elements affects the boundary layer, causing variations in the drag coefficient. The knowledge of these changes is important in order to understand many aspects of flows in nature, and to better control some industrial processes involving turbulent flows. Roughness have been studied for more than a century, dealing, for example, with pressure losses on water channels. One of the most cited works on this topic was published by Nikuradse in 1933, where he describes experiments on sand-roughened pipes measuring how roughness increases drag and skin friction on internal flows. Although it is not a recent problem, studies on turbulent boundary layers over rough elements are still of importance. For example, the characteristic length scales that could proper describe all the boundary layer is an open problem (Jimenez, 2004). The perturbation of the boundary layer by rough elements introduces new scales in the problem, and the velocity and stress profiles are important parameters to understand the influence of the roughness on the main flow.

In the last decades, many researchers turned their attention to turbulent boundary layers over longitudinal grooves, as these rough elements, instead of increasing drag in pipes or channels, may cause a reduction of the surface drag (Djenidi *et al.*, 1994). Those drag reductions can be very useful in several industrial applications, as for reducing the energy demand for pumping oil across large distances, reducing skin fraction over swimming suits, and several other possible applications.

Many studies devoted to the effects of rough elements placed normally to the flow direction have also been conducted over the last decades (Djenidi *et al.*, 1994; Jimenez, 2004; Leonardi *et al.*, 2007). Among the profiles investigated, there are the square and rectangular elements placed normally to the flow direction, regularly separated from each other, that give rise to what is called d- and k-type roughness (Leonardi *et al.*, 2007).

This paper presents an experimental investigation on the transition of a turbulent boundary layer from a smooth to a rough wall, and back to the smooth one. Two-dimensional PIV (Particle Image Velocimetry) measurements of a turbulent boundary layer in the transitions between smooth and rough walls were performed. The flow over the smooth wall was a fully-developed turbulent channel flow in hydraulic smooth regime. For the transition between smooth and rough surfaces,

two rough walls were used. The rough wall consisted of 20 rough elements of rectangular cross section, one rough wall having length between elements, w, of 2 mm and height of elements, k, of 2 mm, and the other having w = 3 mm and k = 2 mm. In both cases, the end of a rough element is 2 mm distant from the beginning of the following one. The rough walls for which $w = k = 2$ mm are assumed to be of d-type (Leonardi *et al.*, 2007; Djenidi *et al.*, 1994), i.e., when the flow outside the roughness becomes isolated from the flow inside the cavities, and the boundary layer is a function of geometric parameters of the channel and the pipe, such as their height or diameter, respectively. The rough walls for which $w > k$ are assumed to be of k-type, with the boundary layer properties depending on the height of elements k (Leonardi *et al.*, 2007).

From the experimental data, it was possible to analyze the properties of the flow over the transition from smooth to rough walls, and back to the smooth one. From the PIV images, the instantaneous velocity fields were computed by cross-correlation using the PIV controller software. Then, using Matlab scripts written by the authors, the mean velocities and fluctuations were computed, and the second order moments were time averaged. Finally, the xy components of the Reynolds stress tensor, $-\rho\overline{u'v'}$, the viscous stress over the transition, $\mu\frac{\partial\bar{u}}{\partial y}$, and the turbulence production, P, were computed, where $\bar{u}$ represents the mean velocity (in time and in space), u' and v' are, respectively, the longitudinal and vertical components of the velocity fluctuations, ρ is the fluid density and μ is the dynamic viscosity. The experimental setup and the main results are presented next.

2. EXPERIMENTAL SETUP

The experimental device used in this study consists of an 1000 liters water reservoir, 2 centrifugal pumps, a flow straightener consisting of a divergent/convergent nozzle filled with glass spheres with 3 mm of diameter to homogenize the flow at the channel inlet, a 5-m-long acrylic channel with rectangular cross-section measuring 160 mm width by 44 mm high, a settling tank, and a return line, so that the device is a closed loop. The channel test section, where the PIV images were obtained, is 1 m long and starts 40 hydraulic diameters (3 m) downstream of the channel inlet, in order to guarantee that the flow will be fully developed at the beginning of the test section. Figure 1 presents a layout of the test section.

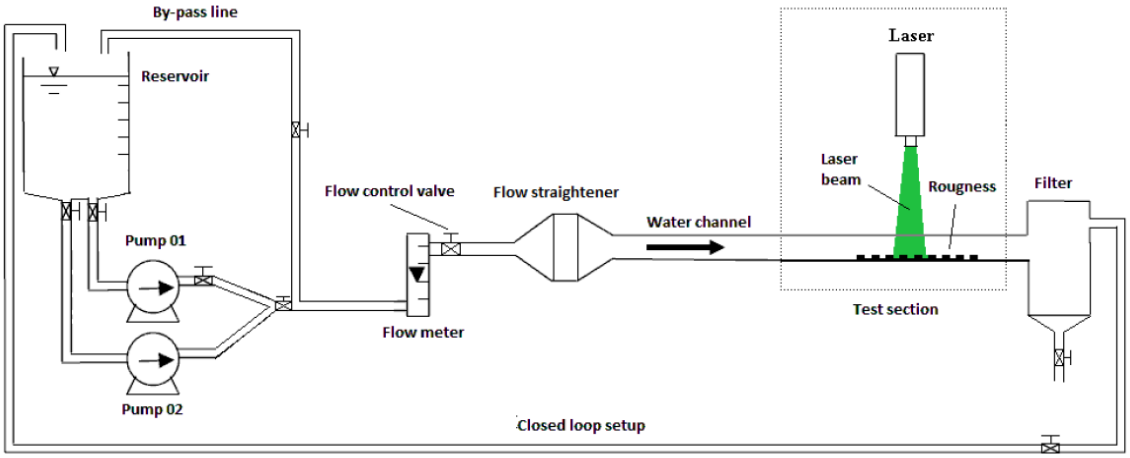

Figure 1: Layout of the experimental device

The CCD camera had a resolution of 2048 $\times$ 2048 pixels. In the CCD, each px^2 corresponds to 7.4 μm $\times$ 7.4 μm, and we used a Nikon AF Micro Nikkor 60 mm f/2.8D lens. The light source was a dual cavity Nd:YAG laser, Q-switched model, emitting, each, 130 mJ of energy by pulse, and pulsing with a maximum frequency of 15 Hz. The laser energy was fixed around 70 % of its maximum energy in order to minimize undesirable reflection from the walls. Each image was obtained using double frames and the instantaneous fields were obtained by cross-correlation.

The camera field of view was of 70 mm x 70 mm. The interrogation area was of 16 px $\times$ 16 px, with an overlap of 50% between the first and the second frames. With the employed interrogation area, field of view, and overlap, 256 interrogation zones of 0.27 mm x 0.27 mm were obtained, corresponding to 256^2 velocity vectors for each test run. Because the total length of the region consisting of smooth, transition, rough, transition and smooth walls was larger than the field of view, the camera was displaced horizontally for each employed flow rate using a rail controlled by the PIV controller software.

Flat plates 6 mm thick made of PVC were inserted in the 3 m entrance length and in the 1 m final length of the channel, covering its bottom and reducing its height to 44 mm. Two rough walls were used in the test section, each one consisting of 20 rough elements of rectangular cross section. One of then had w = 2 mm and k = 2 mm, and the other w = 3 mm and

k = 2 mm. The employed flow rates were of 8 m^3/h and 10 m^3/h, which correspond to Reynolds numbers $Re = \langle U \rangle \, \delta/\nu$ of $7.8 \cdot 10^3$ and $9.6 \cdot 10^3$, respectively, where δ is considered as the half-distance between the surface of the PVC plates and the top wall of the channel, U is the cross-section mean velocity and ν is the kinematic viscosity.

3. RESULTS

Figure 2a presents some results of the mean velocity profiles along different parts of the transition. From this figure, it can be seen that the flow velocity changes in regions close to the wall during the transition, becoming higher when compared to a same vertical position over the smooth wall.

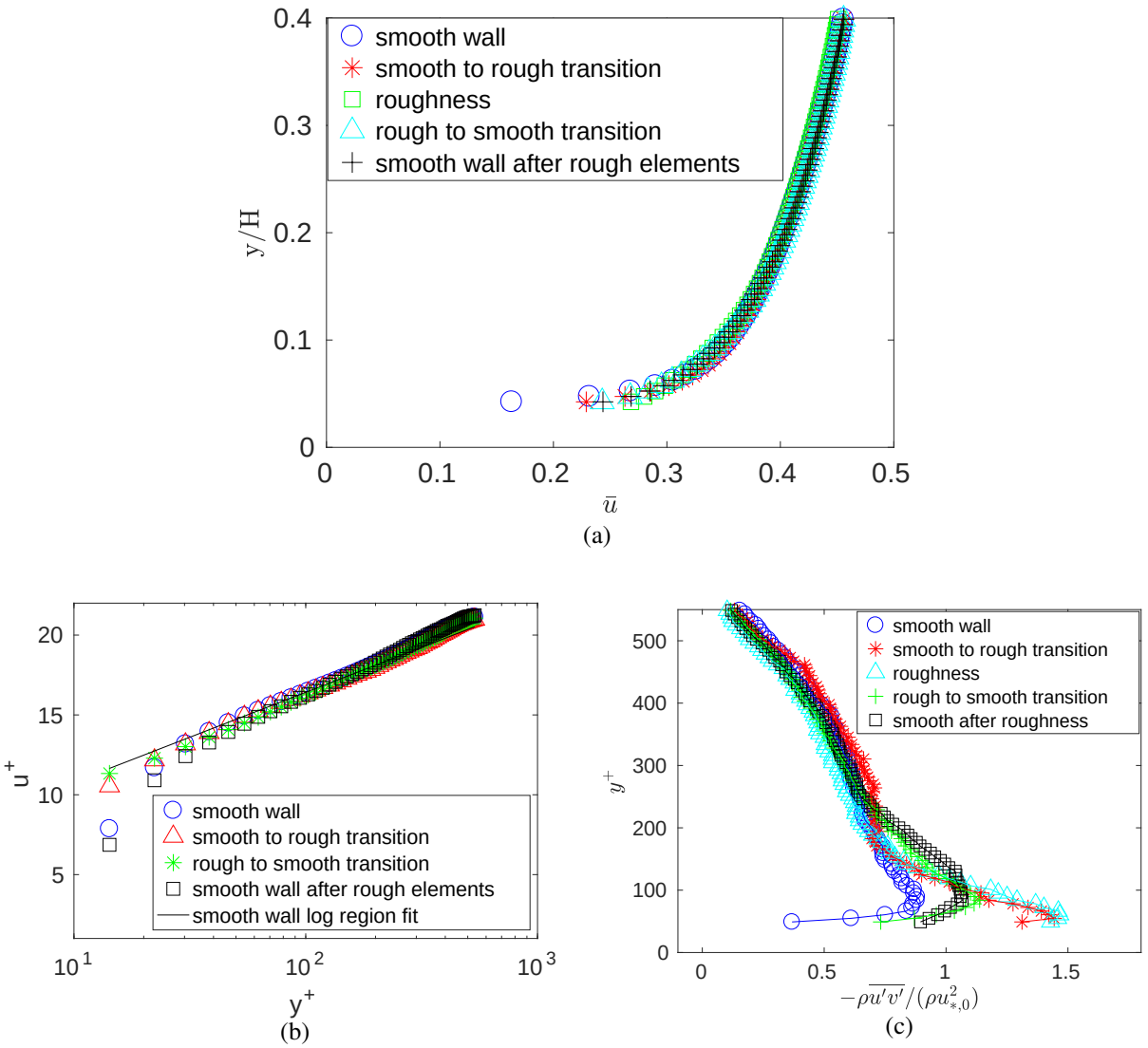

Figure 2: Mean velocities $\bar{u}$ along the transition with (a) 2 mm $\times$ 2 mm and $Re = 9.6 \cdot 10^3$; (b) 3 mm $\times$ 2 mm and $Re = 7.8 \cdot 10^3$, and (c) Reynolds stress $-\rho\overline{u'v'}/\rho u^2_{*,0}$ along the transition for $Re = 9.6 \cdot 10^3$, where $u_{*,0}$ is the shear velocity over the smooth surface.

Figure 2b shows that differences in the velocity profiles are noticeable in the region $y^+ < 100$ (valid for both roughness cases), where $y^+ = y u_* / \nu$ and u_* is the shear velocity. In this study, the wake region (considering the flow above the smooth wall) starts at $y^+ \approx 150$ (the beginning of the wake region was estimated as $y^+ \approx 0.1 Re_\tau$, where τ is the shear stress). The influence of both rough elements, though, was not perceptible above the inner layers.

The velocity plotted in semi-logarithmic scales did also show to be a good parameter to study the differences along the transition. The Reynolds stress component $-\rho\overline{u'v'}$ along the transition does also increase above the roughness, as shown in Fig. 2c, indicating that the presence of rough elements increases the momentum transfers within flow.

The maximum values of $-\rho\overline{u'v'}/\rho u^2_{*,0}$ along the transition with rough elements of 3 mm $\times$ 2 mm, presented in Fig. 3a, show an interesting oscillatory pattern with characteristic length scale of $5w < \lambda < 7w$, where $u_{*,0}$ is the shear velocity over the smooth surface. Although the amplitude of the oscillations changes with the Reynolds number, their

frequency (and characteristic wavelength) did show to be the same for both analyzed flow rates.

This same oscillatory pattern was not observed over the profile with rough elements measuring 2 mm $\times$ 2 mm. Figure 3b shows the maximum values of $-\rho\overline{u'v'}/\rho u_{*,0}^2$, which present a peak downstream of the end of the rough elements, at the transition from the rough back to the smooth wall. The peak is possibly due to more stable vortices that are generated inside the cavities (corresponding to d-type elements) and are shed to the main flow less frequently than in the k-type case. Those shed vortices are advected to the position where the peak is observed ($\approx$ 16 mm downstream of end of the rough wall). It is important to note that, for both cases (k- and d-types), the mean values of $-\rho\overline{u'v'}/\rho u_{*,0}^2$ along the transitions are higher than those above the smooth wall.

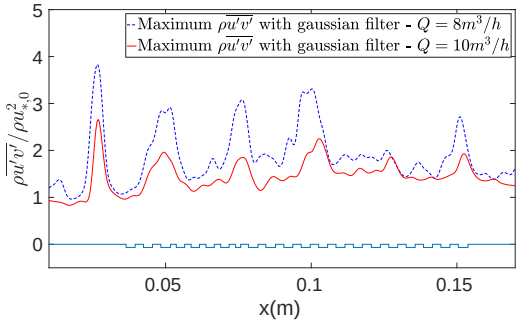

(a)

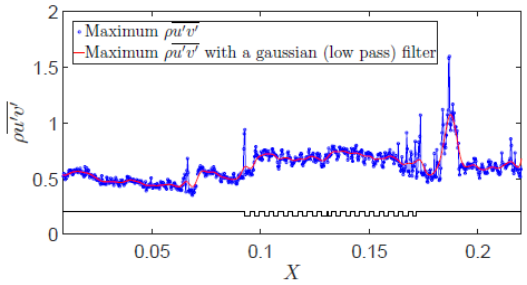

(b)

Figure 3: Maximum values of $-\rho\overline{u'v'}$ along the transition (a) Gaussian filtered signal of the maximum values of $-\rho\overline{u'v'}$ over the 3 mm $\times$ 2 mm rough elements profile for both Reynolds numbers; (b) with square cross section of 2 mm $\times$ 2 mm and $Re = 9.6 \cdot 10^3$

Figure 4 shows that the viscous stress $\left(\mu\frac{\partial\bar{u}}{\partial y}\right)$ close to the wall becomes smaller compared to the same vertical position over the smooth wall. This behavior can be seen in Fig.4b, where the maximum value of $\mu\frac{\partial\bar{u}}{\partial y}/\rho u_{*,0}^2$ is shown along the transition. Although this reduction was observed for both roughness types, over the d-type it was more intense. Figure 4a shows that $\mu\frac{\partial\bar{u}}{\partial y}$ collapses to the same values in the region $y^+ > 100$, i.e., its influence is not noted above the overlap layer.

The reduction of $\mu\frac{\partial\bar{u}}{\partial y}$ over the rough wall can be explained by the change from a non slip condition over the smooth wall, to a partial slip over the rough wall, i.e., over the rough wall the flow alternates between a non slip condition over the top of rough elements and a slip condition above the cavities. The fluid velocity above the cavities corresponds to the tangential velocity of inner-cavities vortices.

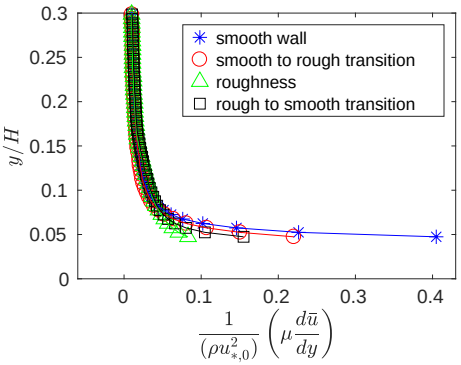

(a)

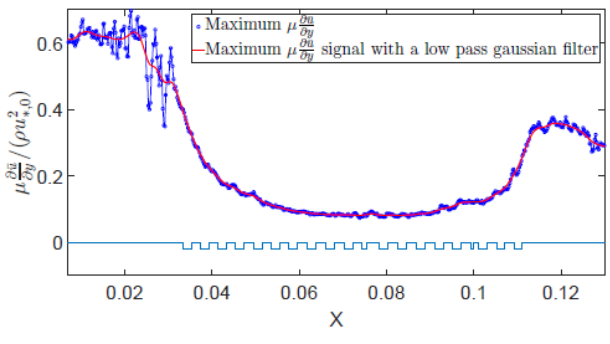

(b)

Figure 4: (a) Viscous stress $\mu\frac{\partial\bar{u}}{\partial y}$ along the transition with rectangular cross section of 2 mm $\times$ 2 mm, $Re = 7.8 \cdot 10^3$; (b) Maximum values of $\mu\frac{\partial\bar{u}}{\partial y}$ along the 3 mm $\times$ 2 mm rough elements, $Re = 9.6 \cdot 10^3$

It is interesting to note that downstream of the rough wall the maximum viscous stress does not assume the same values that it had upstream of the rough wall. This may occur due to vortex shedding from the cavities to the main flow, and their subsequent advection to regions downstream of the rough wall.

The xy component of the turbulence production was computed as

$$P = -\overline{u'v'}\frac{\partial\overline{u}}{\partial y} \tag{1}$$

The maximum turbulence production, P, is a stronger function of $\overline{u'v'}$ than of $\mu\frac{\partial\bar{u}}{\partial y}$. Because the behavior of P and $\overline{u'v'}$ are very similar, no figure is presented here for P. For the k-type roughness, P did show peaks at the same positions as those of the maxima of $-\rho\overline{u'v'}$, also with a characteristic length scale of $5w < \lambda < 7w$.

4. CONCLUSIONS

This paper was devoted to the flow over transitions from smooth to rough walls. It was possible to analyze the mean velocity profiles along the transition and conclude that they do increase close to the wall for the d-type roughness compared to the smooth wall, when compared at the same y positions. For the k-type roughness, the velocity becomes smaller. We did not note a significant effect of the rough elements on the mean velocity profiles above the inner layers of the boundary layer.

The rough elements do increase the Reynolds stress component $-\rho\overline{u'v'}$ above the roughness compared to the smooth wall. A peak on the maxima Reynolds stress was noted downstream of the rough wall for the d-type roughness, while clear oscillations with characteristic length scale of $5w < \lambda < 7w$ were observed for the maximum values of $-\rho\overline{u'v'}$ for the k-type roughness.

The viscous stress close to the wall along the transition became smaller than the viscous stress over the smooth wall when compared at the same y positions. No influence of the rough elements on the viscous stress was observed in the region $y^+ > 100$.

5. ACKNOWLEDGEMENTS

The authors are grateful to ANP, Repsol, Cepetro, Labpetro, CNPq (grant no. 471391/2013-1), and to FAPESP (grants nos. 2012/19562-6 and 2016/13474-9) for the provided financial support.

6. REFERENCES

Djenidi, L., Antonia, R.A. and Anselmet, F., 1994. "LDA measurements in a turbulent boundary layer over a d-type rough wall". *Experiments in Fluids*, Vol. 16, No. 5, pp. 323–329. ISSN 07234864. doi:10.1007/BF00195431.

Jimenez, J., 2004. "Turbulent Flows Over Rough Walls". *Annual Review of Fluid Mechanics*, Vol. 36, No. 1, pp. 173–196. ISSN 0066-4189. doi:10.1146/annurev.fluid.36.050802.122103.

Leonardi, S., Orlandi, P. and Antonia, R.a., 2007. "Properties of d- and k-type roughness in a turbulent channel flow". *Physics of Fluids*, Vol. 19, No. 12, pp. 1–6. ISSN 10706631. doi:10.1063/1.2821908.

Nikuradse, J., 1933. "Laws of flow in rough pipe". *VDI Forschungsheft, In translation, NACA TM 1292*.

7. RESPONSIBILITY NOTICE

The authors are the only responsible for the printed material included in this paper.